



Virtual Monochromatic Image Quality from Dual-Layer Dual-Energy Computed Tomography for Detecting Brain Tumors

Sudharsan S

Assistant Professor, School of Science and Computer Studies, CMR University, Bangalore

Abstract: To evaluate the usefulness of virtual monochromatic images (VMIs) obtained using dual-layer dual-energy CT (DL-DECT) for evaluating brain tumors.

Materials and Methods: This retrospective study included 32 patients with brain tumors who had undergone non-contrast head CT using DL-DECT. Among them, 15 had glioblastoma (GBM), 7 had malignant lymphoma, 5 had high-grade glioma other than GBM, 3 had low-grade glioma, and 2 had metastatic tumors. Conventional polychromatic images and VMIs (40–200 keV at 10 keV intervals) were generated. We compared CT attenuation, image noise, contrast, and contrast-to-noise ratio (CNR) between tumor and white matter (WM) or grey matter (GM) between VMIs showing the highest CNR (optimized VMI) and conventional CT images using the paired *t* test. Two radiologists subjectively assessed the contrast, margin, noise, artifact, and diagnostic confidence of optimized VMIs and conventional images on a 4-point scale.

Results: The image noise of VMIs at all energy levels tested was significantly lower than that of conventional CT images ($p < 0.05$). The 40-keV VMIs yielded the best CNR. Furthermore, both contrast and CNR between the tumor and WM were significantly higher in the 40 keV images than in the conventional CT images ($p < 0.001$); however, the contrast and CNR between tumor and GM were not significantly different ($p = 0.47$ and $p = 0.31$, respectively). The subjective scores assigned to contrast, margin, and diagnostic confidence were significantly higher for 40 keV images than for conventional CT images ($p < 0.01$). **Conclusion:** In head CT for patients with brain tumors, compared with conventional CT images, 40 keV VMIs from DL-DECT yielded superior tumor contrast and diagnostic confidence, especially for brain tumors located in the WM.

Keywords: Brain neoplasms; Tomography, X-ray computed; Radiography, Dual-energy scanned projection; Image enhancement

I. INTRODUCTION

Detecting brain tumors in the early stages is important because prognosis depends on tumor progression, such as size and location [1]. While the gold standard for brain tumor diagnosis remains detection by contrast-enhanced brain MRI, relatively long scanning time under emergent conditions becomes a problem, along with the risk of side effects due to contrast media use [2]. In contrast, CT has the advantages of faster scan times, widespread availability, and low cost. Therefore, brain CT is frequently chosen as the first imaging modality for diagnosing intracranial disease. However, depending on the properties of the tumor, conventional CT may occasionally fail to depict a brain tumor because of lower contrast with the surrounding tissue,

Dual-energy CT (DECT) images are derived by a combination of two separate polychromatic image data, which enables the creation of virtual monochromatic images (VMIs) at arbitrary energy (KeV) levels and material-specific images such as iodine density images [3-6]. VMIs represent a simulation of the attenuation behavior of an ideal monochromatic X-ray beam, and they can better suppress both beam-hardening and energy-shift phenomena compared with conventional polychromatic CT images [7-10]. Thus, VMIs can be used to obtain constituent images of varying contrasts by changing the monochromatic energy levels.

DECT can potentially improve the detection of brain tumors, and a few reports on DECT use for brain tumors have been published [11]. However, to the best of our knowledge, information on the suitability of VMIs and optimal energy levels for the diagnosis of brain tumors has not been established [12-16]. Therefore, this study aimed to evaluate the usefulness of VMIs acquired using dual-layer (DL) DECT for diagnosing brain tumors and to identify the optimal energy levels for detecting brain tumors.



II. MATERIALS AND METHODS

This retrospective study was approved by the Institutional Review Board, and the need for informed consent was waived (IRB No. 1367).

Patients

We retrospectively screened and identified 34 patients with brain tumors who had undergone plain head DL-DECT (IQon Spectral CT; Philips Healthcare) between March 2017 and June 2018 for potential inclusion in this study. Among them, 2 patients with meningioma and schwannoma were excluded to not include patients with tumors outside the brain parenchyma in the study. Data from the remaining 32 cases comprising 18 men and 14 women (mean age, 65.5 years; range, 34–85 years) with body weights ranging from 38.7 to 87.8 kg (mean, 60.6 kg) were used for analyses in this study. Of the 32 patients with tumors, 15 had glioblastoma (GBM), 7 had malignant lymphoma, 5 had high-grade glioma other than GBM, 3 had low-grade glioma, and 2 had metastatic tumor. Of these 32 patients with tumors, 29 were diagnosed pathologically, whereas 3 were diagnosed based on clinical background and additional or follow-up imaging, including MRI. Brain tumors with tumor sizes ranging from 1.3 to 7.5 cm (mean, 4.2 cm) were located in the cerebrum in 28 cases, the brain stem in 2 cases, and the cerebellum in 2 cases.

CT Scanning Protocols

The parameters for non-contrast head CT imaging were detector collimation 64 x 0.625 mm, 500 ms tube rotation time, and 0.298 helical pitch (beam pitch). The tube voltage was 120-kVp with a tube current of 268 mA. The head was scanned from the foramen magnum to the end of the skull in a caudocranial direction. The mean CT dose index volume was 76.1 mGy.

CT Image Reconstruction

Spectral image data were post-processed at a dedicated workstation (Spectral Diagnostic Suite; Philips Healthcare) to generate VMIs at 17 different energy levels (range 40–200 keV at 10 keV intervals) with a spectral level of 1. We used iterative reconstruction-reconstructed conventional CT images (iDose level 1; Philips Healthcare) as controls. The slice thickness of the head CT was 1 and 5 mm, and 1 mm images were used for analyses.

Quantitative Image Analysis

A radiologist with 21 years of experience with neuroimaging quantitatively analyzed the VMIs and conventional CT images. A circular region of interest (ROI) of approximately 25 mm² was placed on each anatomic area to measure the CT attenuation of grey matter (GM; ROI_{GM}), white matter (WM; ROI_{WM}), and brain tumor (ROI_{tumor}), while carefully avoiding neighboring tissue and cerebrospinal fluid. The ROI_{GM} was placed in the putamen, while the ROI_{WM} was placed contralateral to the normal WM of the tumor to exclude edema of the tumor from the ROI. Image noise was defined as the standard deviation (SD) of the ROI_{WM}. The GM-WM contrast was calculated as the difference between CT attenuation of GM and WM. The contrast-to-noise ratio (CNR) was calculated using the following formula:

$$\text{CNR}_{\text{GM-WM}} = (\text{ROI}_{\text{GM}} - \text{ROI}_{\text{WM}}) / \text{image noise}$$

$$\text{CNR}_{\text{tumor-WM}} = (\text{ROI}_{\text{tumor}} - \text{ROI}_{\text{WM}}) / \text{image noise}$$

$$\text{CNR}_{\text{tumor-GM}} = (\text{ROI}_{\text{tumor}} - \text{ROI}_{\text{GM}}) / \text{image noise}$$

We defined the optimized energy VMI as that which resulted in images with the highest CNR. We compared attenuation, image noise, contrast, and CNR between VMIs at the optimized energy level and conventional CT images.

Qualitative Image Analysis

We also performed a qualitative image analysis of the optimized energy VMI and conventional CT images. We used the standard brain window setting (window level, 35 Hounsfield unit [HU]; window width, 80 HU) and adjusted the window level and width as needed during the qualitative assessment.

Two board-certified radiologists with 8 and 10 years of experience in neuroimaging, respectively, used a 4-point subjective scale to independently score the image quality with regard to noise, contrast, margin, artifact, and diagnostic confidence of tumor detection. Both optimized energy level VMIs and conventional CT images were scored. Both readers were blinded to the reconstruction technique and evaluated a randomized CT dataset.

The contrast was evaluated between the tumor and its surrounding tissue, and the margin was assessed as the clarity of the tumor margins. Diagnostic confidence of tumor detection was evaluated as a positively suspected lesion in the tumor region. The scores for contrast, margin, and diagnostic confidence were 1 (unacceptable), 2 (suboptimal, but acceptable), 3 (good), or 4 (excellent).



Noise and artifacts were scored as grade 1 (poor), grade 2 (evaluative with moderate artifacts, acceptable for routine clinical diagnosis), grade 3 (good with minor artifacts, good diagnostic quality), and grade 4 (excellent, no artifacts, unrestricted evaluation). Interobserver disagreement was resolved by consensus.

Statistical Analysis

All statistical analyses were performed using Python programming software (version 3.6.3). Numerical values are expressed as the mean \pm SD. Quantitative image analysis using the paired *t*-test was performed to compare optimized VMIs and conventional CT images. In qualitative image analysis, all scores between the optimized VMIs and conventional CT images were compared using the Wilcoxon signed-rank test. To evaluate the interobserver agreement in the qualitative analysis, we used the following interpretation of the kappa coefficients: < 0.20 = slight, 0.21 – 0.40 = fair, 0.41 – 0.60 = moderate, 0.61 – 0.80 = good, and 0.81 – 1.00 = excellent. *P* value < 0.05 was considered statistically significant.

III. RESULTS

Quantitative Image Analysis

Image noise in VMIs increased with decreasing energy levels (Fig. 1A); however, even 40 keV image noise (5.5 ± 1.4) which was the highest of all the energy levels tested was significantly lower than image noise (5.8 ± 1.2) of conventional CT images ($p = 0.03$) (Fig. 1B). In VMIs, attenuation in the GM, the WM, and the brain tumor increased as the energy level decreased (Fig. 2A). Similarly, all CNRs and contrast between GM-WM, tumor-WM, and tumor-GM of VMIs increased as the energy level decreased (Fig. 2B, C). CNRs of the 40-keV images were the highest among VMIs at all energy levels tested.

CT attenuation of GM, WM, and tumor at 40 keV was significantly higher than that of conventional CT images ($p < 0.001$, $p = 0.001$, and $p < 0.001$, respectively). Contrast and CNR between tumor and WM at 40 keV were significantly higher than those of conventional CT images ($p < 0.001$)

(Fig. 3); however, there was no significant difference in contrast or CNR between tumor and GM in 40-keV and conventional CT images ($p = 0.47$ and $p = 0.31$). Details of the quantitative image analysis are shown in Table 1.

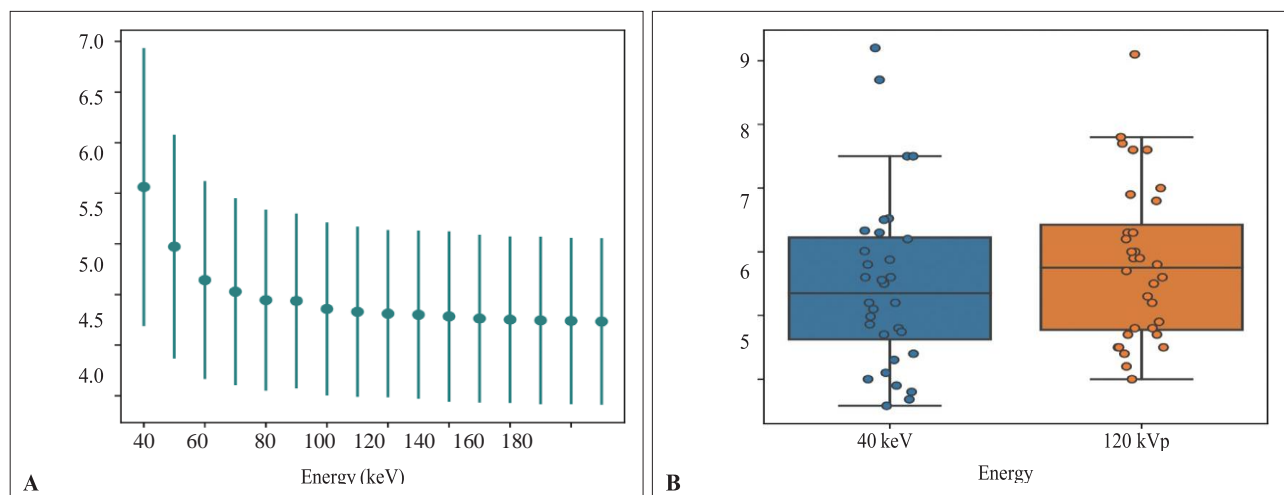


Fig. 1. Image noise according to keV or kVp.

Among all virtual monochromatic images, image noise was the highest in 40-keV images of (A), but it was lower than that of conventional CT images (B). It consists of box representing values of the 1st and the 3rd quartile, separation line inside box representing median value, and two whiskers representing minimum and maximum values. HU = Hounsfield unit

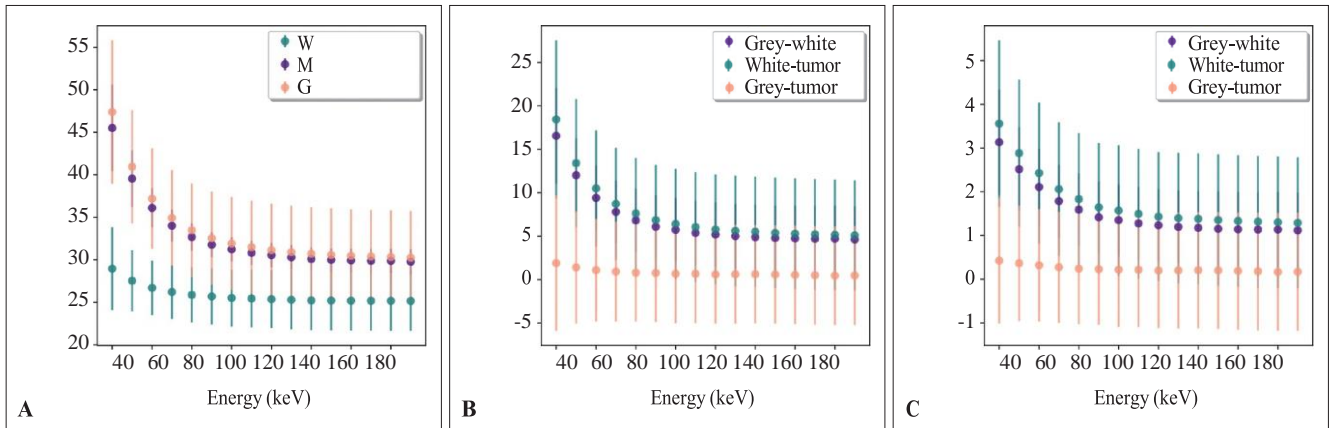


Fig. 2. The CT attenuation (A), contrast (B), and CNR (C) for tumor, WM, and GM in 40-keV images were the highest among all virtual monochromatic images. CNR = contrast-to-noise ratio, GM = grey matter, HU = Hounsfield unit, WM = white matter

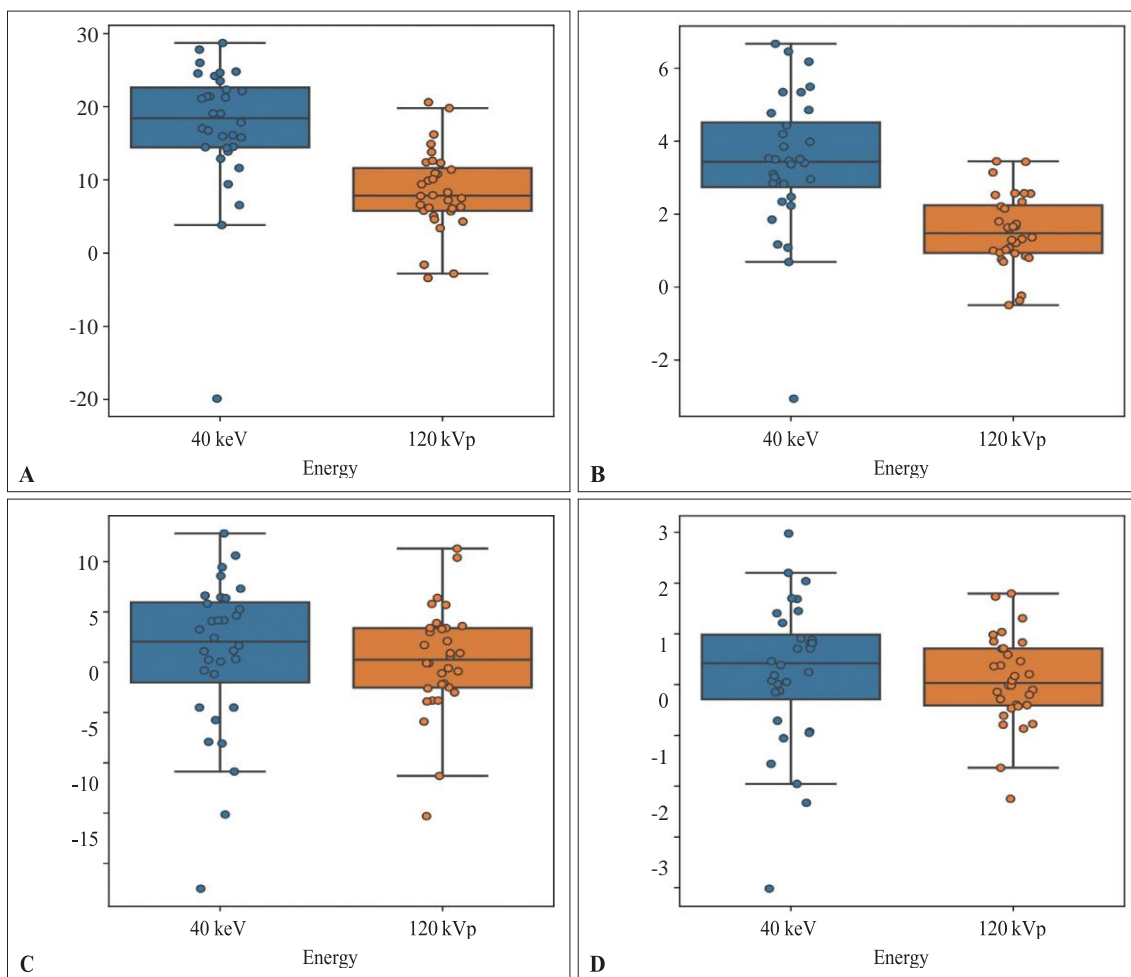


Fig. 3. The contrast and CNR between tumor-WM and those between tumor-GM at 40 keV and 120 kVp.

The contrast (A) and CNR (B) between tumor-WM at 40 keV were significantly higher than those of conventional CT images ($p < 0.001$, $p < 0.001$). However, the contrast (C) and CNR (D) between tumor-GM at 40 keV were not significantly higher than those of conventional CT images ($p = 0.47$, $p = 0.31$).



It consists of a box representing the values of the 1st and the 3rd quartile, the separation line inside the box representing the median value, and two whiskers representing minimum and maximum values. CNR = contrast-to-noise ratio, GM = grey matter, HU = Hounsfield unit, WM = white matter

Qualitative Image Analysis

Table 2 shows the results of the qualitative image analysis. The values assigned to contrast, margin, and diagnostic confidence of tumor detection were significantly higher for 40-keV images than for conventional CT images ($p < 0.001$, $p < 0.001$, and $p = 0.002$, respectively).

In contrast, values assigned to noise and artifact were significantly higher in conventional CT images than in 40-keV images ($p = 0.02$ and $p < 0.001$, respectively). The interobserver agreement on noise, contrast, margin, artifact, and diagnostic confidence of the tumor were found to range between moderate and excellent ($\kappa = 0.423, 0.877, 0.725, 0.735, \text{ and } 0.697$, respectively). Representative cases are shown in Figures 4 and 5.

IV. DISCUSSION

In our analysis of unenhanced head CT images of patients with brain tumors, we showed that optimal VMIs with maximum CNR were obtained at 40 keV.

Furthermore, both contrast and CNR between the tumor and WM in the 40 keV images were significantly higher than those in the conventional CT images ($p < 0.001$).

Conversely, there were no significant differences in contrast and CNRGM-tumor between the 40 keV and conventional CT images. To the best of our knowledge, this is the first study to analyze optimal VMI energy levels in DL-DECT images of brain tumors in non-contrast head CT

Table 1. Quantitative Image Analysis

	40-keV Images	Conventional Images	<i>p</i>
CT attenuation of tumor (HU)	46.4 ± 8.4	34.6 ± 5.4	< 0.001
CT attenuation of WM (HU)	29.2 ± 4.9	26.2 ± 2.8	0.001
CT attenuation of GM (HU)	45.6 ± 5.4	34.4 ± 1.9	< 0.001
Image noise (HU)	5.5 ± 1.4	5.8 ± 1.2	0.03
Contrast of tumor-WM (HU)	17.3 ± 9.0	8.4 ± 5.5	< 0.001
Contrast of tumor-GM (HU)	0.8 ± 7.6	0.2 ± 5.4	0.47
CNR of tumor-WM	3.4 ± 1.9	1.5 ± 1.0	< 0.001
CNR of tumor-GM	0.2 ± 1.4	0.1 ± 0.9	0.31

Data are shown as mean ± standard deviation. CNR = contrast-to-noise ratio, GM = grey matter, HU = Hounsfield unit, WM = whitematter

Table 2. Qualitative Image Analysis

	40-keV Images	Conventional Images	<i>p</i>
Noise	2 (2–2)	2 (2–2.25)	0.02
Contrast	4 (3–4)	3 (3–3.25)	< 0.001
Margin	3 (3–4)	3 (2–3)	< 0.001
Artifact	2 (1–2)	3 (3–3)	< 0.001
Diagnostic confidence of brain tumor detection	4 (3–4)	3 (3–3)	0.002



All parameters were measured on a 4-point scale, with 1 indicating lowest quality and 4 indicating highest quality. Data are shown as median (25–75th percentile).

Our study suggests that low-energy (40 keV) images might be well-suited to delineate tumors in the WM because both contrast and CNRW_M-tumor were superior in these low keV images. This observed superior tissue contrast at lower energy images may be due to the increased photoelectric effect [13,17,18]. The rate of photoelectric absorption in GM is higher than that in WM because WM contains 8% more carbon and 8% less oxygen than GM for myelinization, resulting in a lower effective atomic number of WM compared to that of GM [19].

Additionally, as the energy level decreases in the VMIs, noise increases [7], but we found that image noise in the VMIs at all energy levels tested was significantly lower than that of conventional CT images. These observations are comparable to those from previous reports of lower noise in VMIs compared with that in conventional images in DL-DECT [20,21].

The DL-DECT system simultaneously collects both low-and high-energy data for a given anatomical region using two detector layers. Thus, VMI reconstruction can reduce beam-hardening artifacts and anti-correlated noise in photoelectric and Compton scatter images.

As a result, in low keV images, noise also lowers conventionally, and image quality is considered to be improved. This is an important advantage of DL-DECT imaging, which is not available with rapid-switching DECT or dual-source DECT imaging [21].

Notably, dual-energy CT might not be as effective in delineating GM tumors as it is for WM tumors because contrast and CNR between the GM and tumor in low keV images were not significantly higher than those in conventional images. This is because GM consists predominantly of neuronal cell bodies and dendrites and contains less myelin sheath than WM.

The low keV increased CT attenuation not only in the tumor but also in the GM, thus reducing contrast and CNR. Additionally, even though noise in the 40-keV images was lower in the quantitative analysis ($p = 0.03$), the qualitative analysis showed that both noise and artifact in 40-keV images worsened compared with those in conventional CT images ($p = 0.02$ and $p < 0.001$). Taken together, these observations imply that utilizing low-energy VMIs may not be very effective for tumors located in the GM.

Our study has some limitations. First, the number of cases in this study was small and we could not evaluate the diagnostic performance of VMIs and conventional images for brain tumors that are difficult to visualize on unenhanced CT (e.g., small tumors and low-grade gliomas).

Our results need to be validated in larger scale studies. Second, we were unable to compare the image quality with small intra-axial tumors confined to the cerebral cortex or extra-axial tumors such as meningiomas. Future studies should address these aspects as well. Third, we evaluated the contrast between tumor and normal GM or WM and did not evaluate the contrast between peritumoral low attenuation and GM or WM in this study. It might be possible that the decreased CT numbers of WM in low keV images result in decreased contrast between peritumoral low attenuation and WM, especially for high-grade gliomas.

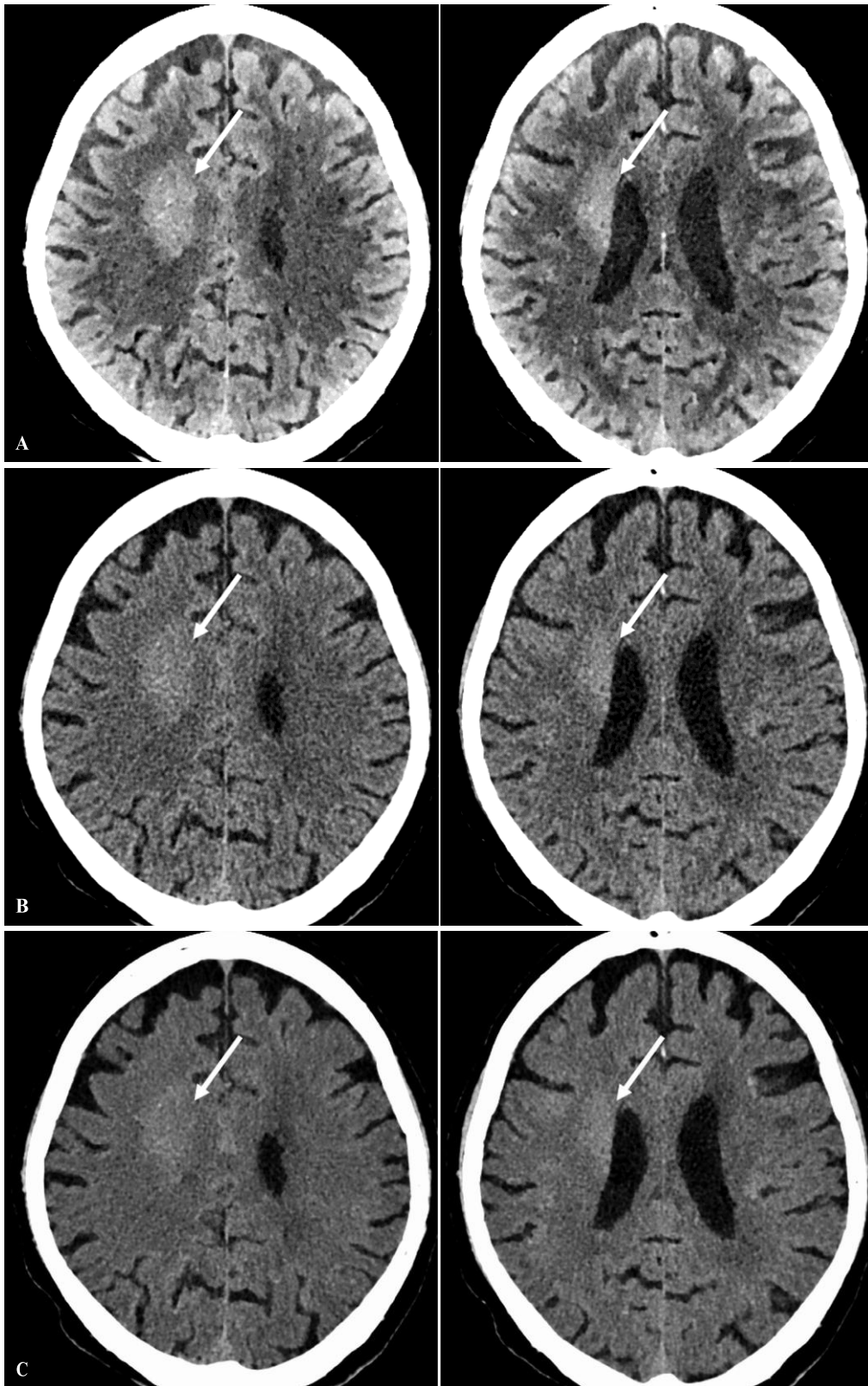


Fig. 4. Images of an 85-year-old woman with diffuse large B-cell lymphoma. The optimized energy level was defined as that resulting in images with the highest contrast-to-noise ratio between tumor (arrows) and white matter (virtual monochromatic images at 40 keV). The contrast of the 40-keV images appeared to be visually superior. **A.** 40 keV image. **B.** 120 kVp image. **C.** 200 keV image.

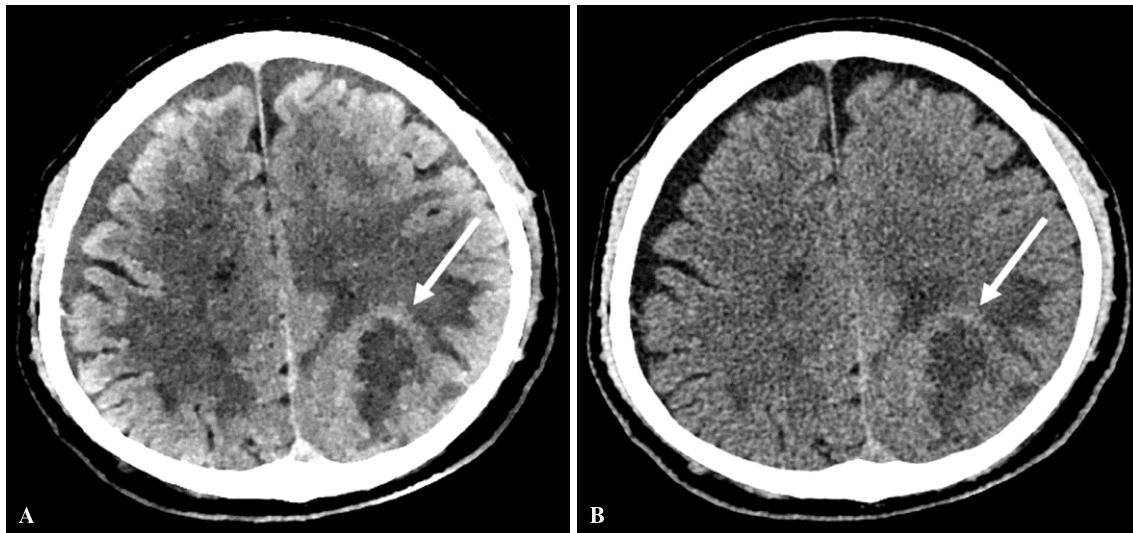


Fig. 5. A 75-year-old man (body weight, 75.6 kg) with suspected intracranial disease underwent brain CT.

The pathological diagnosis was glioblastoma. Images show brain dual-layer dual-energy CT at the level of the center of the brain tumor (arrows) at 40 keV (A) and at 120 kVp (B). The 40-keV image, but not the 120-kVp image, clearly depicts a margin between the tumor and white matter. However, the margin between the tumor and grey matter, and peritumoral low attenuation are unclear.

Further studies are needed to determine the optimal keV to evaluate the extent of tumor invasion. Fourth, we defined optimal keV as that which yielded the highest CNR between the tumor and the brain parenchyma; however, other reports have stated that high-energy monochromatic (190 keV) images may be more reliable than standard 120 kV images for detecting intracranial hemorrhages [22]. While we show that high keV images have lower contrast between the WM and tumor, it may also reduce noise and artifacts. Nonetheless, we cannot rule out the possibility that, compared with low keV images, high keV images would be well-suited to delineate tumors at the brain surface and at the cranial base. Further investigations will be necessary to address these aspects.

V. CONCLUSION

In conclusion, in non-contrast head CT for patients with brain tumors, 40 keV VMIs from DL-DECT images offer superior tumor contrast and diagnostic confidence for detecting brain tumors than conventional CT images, especially in WM brain tumors.

Conflicts of Interest

The authors have no potential conflicts of interest to disclose.

Author Contributions

Conceptualization: Takeshi Nakaura. Data curation: Shota Tanoue. Formal analysis: Takeshi Nakaura. Investigation: Shota Tanoue. Methodology: Takeshi Nakaura. Project administration: Osamu Ikeda. Resources: Hiroyuki Uetani. Software: Takeshi Nakaura. Supervision: Yasuyuki Yamashita. Validation: Yasunori Nagayama. Visualization: Shota Tanoue. Writing—original draft: Shota Tanoue. Writing—review & editing: Takeshi Nakaura.

ORCID iDs

Shota Tanoue

<https://orcid.org/0000-0002-5516-1747>

Takeshi Nakaura

<https://orcid.org/0000-0002-9010-0341>

Yasunori Nagayama

<https://orcid.org/0000-0003-3280-7346>

Hiroyuki Uetani

<https://orcid.org/0000-0002-0547-1210>

Osamu Ikeda

<https://orcid.org/0000-0001-9128-1431>

Yasuyuki Yamashita

<https://orcid.org/0000-0002-2905-1093>



REFERENCES

- [1]. Capellades J, Puig J, Domenech S, Pujol T, Oleaga L, Camins A, et al. Is a pretreatment radiological staging system feasible for suggesting the optimal extent of resection and predicting prognosis in glioblastoma? An observational study. *J Neurooncol* 2018;137:367-377
- [2]. Leung D, Han X, Mikkelsen T, Nabors LB. Role of MRI in primary brain tumor evaluation. *J Natl Compr Canc Netw* 2014;12:1561-1568
- [3]. Lennartz S, Laukamp KR, Neuhaus V, Große Hokamp N, Le Blanc M, Maus V, et al. Dual-layer detector CT of the head: initial experience in visualization of intracranial hemorrhage and hypodense brain lesions using virtual monoenergetic images. *Eur J Radiol* 2018;108:177-183
- [4]. Kamalian S, Lev MH, Pomerantz SR. Dual-energy computed tomography angiography of the head and neck and related applications. *Neuroimaging Clin N Am* 2017;27:429-443
- [5]. Kamalian S, Lev MH, Pomerantz SR. Dual-energy computed tomography angiography of the head and neck and related applications. *Neuroimaging Clin N Am* 2017;27:429-443
- [6]. Paul J, Bauer RW, Maentele W, Vogl TJ. Image fusion in dual energy computed tomography for detection of various anatomic structures--effect on contrast enhancement, contrast-to-noise ratio, signal-to-noise ratio and image quality. *Eur J Radiol* 2011;80:612-619
- [7]. Hsu CC, Kwan GN, Singh D, Pratap J, Watkins TW. Principles and clinical application of dual-energy computed tomography in the evaluation of cerebrovascular disease. *J Clin Imaging Sci* 2016;6:27
- [8]. Wu R, Watanabe Y, Satoh K, Liao YP, Takahashi H, Tanaka H, et al. Quantitative comparison of virtual monochromatic images of dual-energy computed tomography systems: beam hardening artifact correction and variance in computed tomography numbers: a phantom study. *J Comput Assist Tomogr* 2018;42:648-654
- [9]. Naruto N, Itoh T, Noguchi K. Dual-energy computed tomography for the head. *Jpn J Radiol* 2018;36:69-80
- [10]. Kamiya K, Kunimatsu A, Mori H, Sato J, Akahane M, Yamakawa T, et al. Preliminary report on virtual monochromatic spectral imaging with fast kVp switching dual energy head CT: comparable image quality to that of 120-kVp CT without increasing the radiation dose. *Jpn J Radiol* 2013;31:293-298
- [11]. Lin XZ, Miao F, Li JY, Dong HP, Shen Y, Chen KM. High-definition CT Gemstone spectral imaging of the brain: initial results of selecting the optimal monochromatic image for beam-hardening artifacts and image noise reduction. *J Comput Assist Tomogr* 2011;35:294-297
- [12]. Kim SJ, Lim HK, Lee HY, Choi CG, Lee DH, Suh DC, et al. Dual-energy CT in the evaluation of intracerebral hemorrhage of unknown origin: differentiation between tumor bleeding and pure hemorrhage. *AJNR Am J Neuroradiol* 2012;33:865-872
- [13]. Hwang WD, Mossa-Basha M, Andre JB, Hippe DS, Culbertson S, Anzai Y. Qualitative comparison of non-contrast head dual-energy computed tomography using rapid voltage switching technique and conventional computed tomography. *J Comput Assist Tomogr* 2016;40:320-325
- [14]. Park J, Choi YH, Cheon JE, Kim WS, Kim IO, Pak SY, et al. Advanced virtual monochromatic reconstruction of dual-energy unenhanced brain computed tomography in children: comparison of image quality against standard mono-energetic images and conventional polychromatic computed tomography. *Pediatr Radiol* 2017;47:1648-1658
- [15]. Pomerantz SR, Kamalian S, Zhang D, Gupta R, Rapalino O, Sahani DV, et al. Virtual monochromatic reconstruction of dual-energy unenhanced head CT at 65-75 keV maximizes image quality compared with conventional polychromatic CT. *Radiology* 2013;266:318-325
- [16]. Hixson HR, Leiva-Salinas C, Sumer S, Patrie J, Xin W, Wintermark M. Utilizing dual-energy CT to improve CT diagnosis of posterior fossa ischemia. *J Neuroradiol* 2016;43:346-352
- [17]. Yu L, Christner JA, Leng S, Wang J, Fletcher JG, McCollough CH. Virtual monochromatic imaging in dual-source dual-energy CT: radiation dose and image quality. *Med Phys* 2011;38:6371-6379
- [18]. Nagayama Y, Nakaura T, Tsuji A, Urata J, Furusawa M, Yuki H, et al. Radiation dose reduction using 100-kVp and a sinogram-affirmed iterative reconstruction algorithm in adolescent head CT: impact on grey-white matter contrast and image noise. *Eur Radiol* 2017;27:2717-2725
- [19]. Park JE, Choi YH, Cheon JE, Kim WS, Kim IO, Cho HS, et al. Image quality and radiation dose of brain computed tomography in children: effects of decreasing tube voltage from 120 kVp to 80 kVp. *Pediatr Radiol* 2017;47:710-717
- [20]. Brooks RA, Di Chiro G, Keller MR. Explanation of cerebral white--gray contrast in computed tomography. *J Comput Assist Tomogr* 1980;4:489-491
- [21]. Nagayama Y, Nakaura T, Oda S, Utsunomiya D, Funama Y, Iyama Y, et al. Dual-layer DECT for multiphasic hepatic CT with 50 percent iodine load: a matched-pair comparison with a 120 kV protocol. *Eur Radiol* 2018;28:1719-1730
- [22]. SELLERER T, Noël PB, Patino M, Parakh A, Ehn S, Zeiter S, et al. Dual-energy CT: a phantom comparison of different platforms for abdominal imaging. *Eur Radiol* 2018;28:2745-2755
- [23]. Bodanapally UK, Archer-Arroyo KL, Dreizin D, Shanmuganathan K, Schwartzbauer G, Li G, et al. Dual-energy computed tomography imaging of head: virtual high-energy monochromatic (190 keV) images are more reliable than standard 120 kV images for detecting traumatic intracranial hemorrhages. *J Neurotrauma* 2019;36:1375-1381